ARTICLE IN PRESS

Ceramics International xxx (xxxx) xxx-xxx

ELSEVIER

Contents lists available at ScienceDirect

Ceramics International

journal homepage: www.elsevier.com/locate/ceramint



Structural, magnetic and photocatalytic properties of Sr²⁺ doped BiFeO₃ nanofibres fabricated by electrospinning

Rulu Yang, Haibin Sun*, Jiao Li*, Yan'an Li

School of Materials Science and Engineering, Shandong University of Technology, Zibo, Shandong 255049, PR China

ARTICLE INFO

Keywords: Electrospinning BFO nanofibres ${\rm Sr}^{2+}$ doping Magnetic properties Photocatalytic properties

ABSTRACT

 Sr^{2+} doped $BiFeO_3$ ($Bi_{1-x}Sr_xFeO_3$, $0 \le x \le 0.35$) nanofibres were fabricated by a sol-gel based electrospinning method. The as-spun $BiFeO_3$ (BFO) nanofibres consist of fine grained particles with high crystallinity. With Sr^{2+} doping, both the magnetic and photocatalytic properties of BFO are effectively improved. The best photocatalytic property for degradation of the methylene blue (MB) is obtained in $Bi_{0.75}Sr_{0.25}FeO_3$ nanofibres due to their weakest photoluminescence (PL) intensity. Meanwhile, the photocatalytic property of $Bi_{0.75}Sr_{0.25}FeO_3$ nanofibres is much higher than that of nanoparticles with the same constituent, which is attributed to the unique one-dimension fibrous structure benefiting the separation and decreased recombination of e^{\cdot}/h^+ pairs. This work proposes an effective approach for the degradation of organic pollutes.

1. Introduction

BiFeO $_3$ (BFO) is the only known single-phase room temperature multiferroic material due to its high Curie temperature (830 °C) and Neel temperature (370 °C), thus attracting widespread applications in field of data storage, sensors, photovoltaics and spintronics [1–4]. In addition, BFO is also used as an efficient UV and visible light photocatalyst for water splitting and organic pollutants degradation because of its narrow band gap energy [4]. However, the poor magnetic properties of pure bulk BFO inhibit the practical applications, due to its long-range spiral spin modulation structure with a wavelength of \sim 62 nm [2].

Ions (i.e., Ca^{2+} , Sr^{2+} , Pb^{2+} , and Ba^{2+}) doping is mostly employed as an effective approach to enhance the magnetic properties of BFO [2,5,6]. Among these ions, Sr^{2+} is considered more interesting than other divalent substituents, becasue Sr^{2+} doped BFO possess the highest magnetic field induced polarization ($P_r = 96 \ \mu\text{C/cm}^2$ at $10\ T$) among the reported values of BFO with other dopings [7,8]. It is worth to note that Sr^{2+} doped BFO exhibits not only enhanced magnetic properties but also improved photocatalytic properties, thus being regarded as a promising photocatalyst [9].

Another possible approach to enhance the magnetization of BFO is decreasing the particle size to less than 62 nm, aiming to suppress the spiral spin structure. Considerable works are focused on zero-dimensional (0-D) and one-dimensional (1-D) BFO nanostructures, such as thin film, particles, tubular, fibrous [2,10–13].. Compared with the traditional nanoparticles and thin films, 1-D nanostructures promises several advantages including high specific surface area, few crystal

defects, uniform grain sizes, free-agglomeration, reduced recombination probability of electrons and holes, and so on. For instance, Ca²⁺ doped BFO nanofibres fabricated by electrospinning method exhibits both excellent magnetic and photocatalytic performance due to their unique structure [2].

Inspired by above discussions, herein, we fabricated the Sr²⁺ doped BFO nanofibres by electrospinning. And the structure, magnetic and photocatalytic behaviors were investigated in detail.

2. Experimental

 Sr^{2+} doped BFO (Bi1.xSrxFeO3, 0 \leq x \leq 0.35) nanofibres were fabricated by a sol-gel based electrospinning method. All of the chemicals were of analytical grade and used without further purification. Stoichiometric amounts of Bi(NO3)3·5H2O, Fe(NO3)3·9H2O and Sr (NO3)3·9H2O were dissolved in 18.25 mL mixture solution of ethylene glycol monomethyl ether (EGME), ethanol, glacial acetic acid and and N,N-Dimethylformamide (DMF) with a volume ratio of 5:3.75:2.5:7. The metal ion concentration of the mixture solution was 0.1 M. 1.5 g polyvinylpyrrolidone (PVP) was subsequently added into the solution. After a continuous stirring for 24 h, transparent solutions were formed. And then, the electrospinning was processed in a homemade electrospinning unit at 0.4 mL h $^{-1}$ and at 13 kV. The distance between the collector and the needle was 10 cm. Finally, the collected nanofibres were dried at 60 °C for 24 h, followed by thermally annealing at 600 °C for 2 h in air.

The phase composition analysis was characterized by X-ray

E-mail addresses: sunhaibin111@163.com (H. Sun), haiyan9943@163.com (J. Li).

https://doi.org/10.1016/j.ceramint.2018.04.256

Received 9 April 2018; Received in revised form 30 April 2018; Accepted 30 April 2018 0272-8842/ © 2018 Elsevier Ltd and Techna Group S.r.l. All rights reserved.

^{*} Corresponding authors.

R. Yang et al. Ceramics International xxxx (xxxxx) xxxx—xxx

diffraction analysis (XRD, D8 Advance, Bruker AXS, German) with Cu $\rm K_a$ radiation ($\lambda=1.5418$ Å). The microstructures were observed using a field emission scanning electron microscopy (FE-SEM, Sirion 200, FEI, USA) and transmission electron microscopy (TEM, Tecnai G2 F20 S-TWIN, FEI, USA). Magnetic characterization was carried out by a superconducting quantum interference device magnetometer (MPMS XL-7, USA). PL intensities were tested using the photometer (FL4500, Hitachi, Japan). UV–Vis was measured in Hitachi U3310 spectrophotometer in an analysis range of 200–800 nm taking BaSO₄ as the reference material.

The photocatalytic properties of the BFO nanofibres were evaluated by the degradation of methylene blue (MB). 25 mg of BFO nanofibres were added into 300 mL of MB solutions (10 mg L $^{-1}$). Subsequently, the mixtures were placed under the irradiation of simulated sunlight in a dark condition. The degradation of MB was monitored by UV–visible absorption spectroscopy at the wavelength of 666 nm for every 30 min. The degradation efficiency of MB is confirmed by C_x/C_0 , where C_0 and C_x are concentrations of MB solutions before and after irradiation.

3. Results and discussion

3.1. Phase analysis

Fig. 1(a) shows XRD patterns of the as-spun BFO nanofibres. All diffraction peaks are well corresponded to the rhombohedral structure with space group R3c, and reveal high crystallinity. As shown in Fig. 1(b), the peaks of Sr^{2+} doped samples are merged near $2\theta=32^{\circ}$ due to the Sr^{2+} substitution in the host BFO. With Sr^{2+} doping amounts increasing, the peaks shift to higher angles caused by the change of crystal structures. The similar results have been reported in other literatures [2,9,14]. However, it is worth to note that minor low-intensity $Bi_2Fe_4O_9$ impurity peaks around $2\theta=28^{\circ}$ are observed for $x=0.35\,Sr^{2+}$ doped samples, which results from the excess Sr^{2+} doping.

3.2. Microstructures

Shown in Fig. 2(a)–(e) are SEM images of as-spun BFO nanofibres. It can be seen that the undoped BFO sample consists of some short bead-like fibres with unsmooth surfaces and uneven diameters, while continuous and smooth fibres are observed in Sr^{2+} doped BFO samples. With Sr^{2+} doping amounts increasing, the surface becomes smoother and the diameter becomes smaller, this is because that appropriate Sr^{2+} doping inhibits the BFO grain growth during sintering process, which is similar with other reports [2]. The diameter of samples with $x=0.25\,\mathrm{Sr}^{2+}$ doping shrinks to about 100 nm after sintering. However,

the $x=0.35\,{\rm Sr}^{2+}$ doped sample shows an undesired large diameter (~ 300 nm), may be attributed to the minor Bi₂Fe₄O₉ impurity caused by the excess Sr²⁺ doping, as described above.

As shown in Fig. 3, both the undoped and Sr^{2+} doped BFO fibres consist of some fine grained particles with high crystallinity, which is inconsistent with the previous XRD analysis. The measured lattice distance along [100] direction of $x=0.25\,\mathrm{Sr}^{2+}$ doped samples (0.224 nm) is smaller than that of undoped samples (0.280 nm). As known, the ionic radii of Sr^{2+} (1.18 Å) is larger than Bi^{3+} (1.03 Å), so the replacement of Bi^{3+} by Sr^{2+} in BFO cannot explain the decrease of lattice distance. Actually, oxygen vacancies result from the charge compensation caused by the different charge valancies of Bi^{3+} and Sr^{2+} mainly contribute to the decrease of lattice dimensions [14].

3.3. Magnetization

Fig. 4 shows the magnetic hysteresis (M-H) curves of BFO nanofibres with different ${\rm Sr}^{2+}$ doping amounts measured in a magnetic field of 10 kOe at 300 K. Obviously, the ${\rm Sr}^{2+}$ doping effectively improve the magnetization of BFO. The values of saturated magnetization for ${\rm Bi_{0.75}Sr_{0.25}FeO_3}$ (0.45 emu/g) and ${\rm Bi_{0.65}Sr_{0.35}FeO_3}$ (0.57 emu/g) are much higher than that of undoped BFO (0.02 emu/g). The enhancement of magnetization may be attributed to the ${\rm Sr}^{2+}$ doping and nano-effect. Firstly, the oxygen vacancies caused by ${\rm Sr}^{2+}$ substitution suppress the spiral spin structure of BFO, leading to the weak ferromagnetism. Meanwhile, more structure distortion caused by the increase of ${\rm Sr}^{2+}$ doping can suppress cycloid spin structure in BFO [15]. Secondly, nanoparticles with larger surface make the spins more uncompensated because the long-range antiferromagnetic order is interrupted by the surface [9].

3.4. Photocatalytic property

The photoluminescence (PL) spectra of BFO samples measured at room temperatures is shown in Fig. 5, which can be used to characterize the formation, migration and recombination of electron/hole (e^-/h^+) pairs [16]. It can be seen that all samples demonstrate intensity peaks around the wavelength of 545 nm, and the $x=0.25\,\mathrm{Sr}^{2+}$ doped samples have the weakest PL intensity. As reported by Zhang et al., [17] the weaker PL intensity indicates the separation of e^-/h^+ pairs is easily promoted, thus enhancing the photocatalytic activity. Therefore, it can be concluded that the $x=0.25\,\mathrm{Sr}^{2+}$ doped BFO has the best photocatalytic activity.

Organic pollutant MB was used to test the photocatalytic activities of Sr^{2+} doped BFO. The degradation efficiencies of the MB catalysts illuminated for 150 min are shown in Fig. 6. It can be seen that the Sr^{2+}

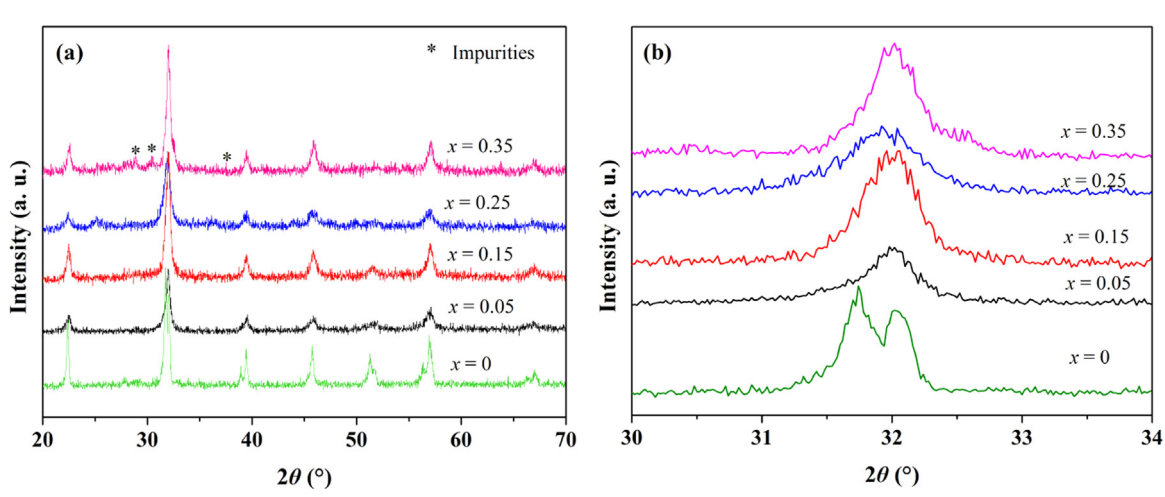


Fig. 1. XRD patterns of (a) BFO nanofibres with different Sr^{2+} doping amounts and (b) magnified XRD patterns for $30^{\circ} \le 20 \le 34^{\circ}$.

Download English Version:

https://daneshyari.com/en/article/7886678

Download Persian Version:

https://daneshyari.com/article/7886678

<u>Daneshyari.com</u>